Can the shape of attractor forbid chaotic phase synchronization?

M. A. Zaks
Institut für Physik, Humboldt-Universität zu Berlin, D-12489 Berlin, Germany

E.-H. Park
Neural Engineering Center, Department of Biomedical Engineering, Case Western Reserve University, Cleveland, Ohio 44106-4912, USA

(Received 20 April 2005; published 23 August 2005)

We address the question, which properties of a chaotic oscillator are crucial for its ability/inability to synchronize with external force or other similar oscillators. The decisive role is played by temporal coherency whereas the shape of the attractor is less important. We discuss the role of coordinate-dependent reparameterizations of time which preserve the attractor geometry but greatly influence the coherency. An appropriate reparameterization enables phase synchronization in coupled multiscroll attractors. In contrast, the ability to synchronize phases for nearly isochronous oscillators can be destroyed by a reparameterization which washes out the characteristic time scale.

DOI: 10.1103/PhysRevE.72.026215 PACS number(s): 05.45.Xt

I. INTRODUCTION

Synchronization, an effect ubiquitous in nature and technology [1], continues to attract the attention of numerous researchers. A multifaceted phenomenon, synchronization has several meanings: this word denotes a situation in which the interacting elements of the ensemble proceed to the identical behavior (*complete* synchronization), a situation in which the instantaneous state of one element becomes a well-defined function of the state of the other one (*generalized* synchronization), a situation in which one element accurately reproduces the dynamics of the other one but shifts it in time (*lag* synchronization) and so on.

Often the interacting oscillatory processes are of a rather different physical (chemical, biological, etc.) nature, and it is difficult to find a common basis for identifying their synchronized features. Since, however, these processes evolve in time, we can compare the pace of oscillations in participating subsystems. Synchronization between the interacting periodic oscillators has been known for centuries; by now we are aware that this notion can be extended to interacting chaotic systems, so that their phases become entrained whereas the amplitudes can remain chaotic and uncorrelated: this is the *chaotic phase* synchronization [2].

Unlike other forms of synchrony, chaotic phase synchronization concerns only one aspect of interaction: adjustment between the rhythms of oscillatory chaotic dynamics. On quantifying dynamics in terms of phases, the adjustment is expressed as boundedness in time of the difference between the phases of chaotic oscillators.

In certain ensembles of chaotic oscillators the state of phase synchronization is established already at very low coupling strength. For other sets of chaotic elements the phases are virtually impossible to synchronize: they diverge irrespective of the coupling intensity.

Recently an attempt was made to explain this property by the geometry of the attractors of interacting systems [3]. Based on the results of numerical experiments with coupled Lorenz systems, the authors of [3] assign the desynchronizing action to the "switching region" between the scrolls of the Lorenz attractor and conclude that "phase synchronization cannot occur in dynamical systems having attractors with multiple scrolls in phase space." In this paper we revisit this problem and demonstrate that the shape of the attractor alone (in particular, the presence of several scrolls) does not decide on synchronizability.

An attracting set is a geometrical object in the phase space. Accordingly, its most straightforward characteristics are measured in terms of lengths, areas, and volumes. The more subtle ones, like fractal dimensions, are expressed through limits of ratios of lengths. The language of phase synchronization, on the other side, is based on measurements of time scales in interacting oscillators.

The same geometrical set can serve as an attractor for different dynamical systems. Since the velocity of motion along the attractor can differ much from a system to another system, it is intuitively clear that the conclusions on the possibility of phase synchronization cannot be drawn solely from geometrical arguments [14].

Below we endow the geometry of two exemplary attractors (the Lorenz attractor and the Rössler attractor) with different types of temporal evolution. By doing this, we transform chaotic dynamics which lacks a sharp characteristic time scale to a rhythmic one and vice versa. The implications of this transition for the onset of phase synchronization between coupled systems will be discussed.

II. TEMPORAL COHERENCY AND REPARAMETERIZATION OF TIME

Behavior in the ensemble of weakly coupled systems is largely predetermined by the properties of uncoupled chaotic elements. Among them, we are particularly interested in purely temporal characteristics. From this point of view, it is convenient to speak about a "cycle" of chaotic oscillations. The cycle can be a time interval between two subsequent maxima of one of the variables, or, in a more general setup,

a time interval between two subsequent returns onto a global secant surface (Poincaré surface) in the phase space. If the oscillatory process is represented as a composition of phase and amplitude, one cycle corresponds to the interval during which the phase acquires an increment of 2π. A long piece of the chaotic trajectory consists of many such cycles and the length of the cycle fluctuates. Here a rough distinction can be made between temporally coherent and noncoherent dynamics. In the former, nearly isochronous case, the fluctuations of the "cycle" duration are small compared to the duration itself, so that the well-defined time scale of oscillations is recognizable. In the latter case, this duration strongly varies. Intuitively one expects that phases of temporally coherent chaotic systems are easier to synchronize than those of the incoherent ones.

The degree of temporal coherency can be inferred from the shape of the power spectrum: A sharp spectral peak which is by several orders of magnitude higher than the immediate background means that dynamics has a well-resolvable characteristic time scale. The broadband power spectrum, on the other hand, is typical for processes which lack temporal coherency.

An alternative description of temporal coherency is delivered by the distribution of periods or frequencies of unstable periodic orbits (UPOs) embedded in the attractor. Here, an appropriate characteristics is the set of individual frequencies of UPOs. Individual frequency is defined for each UPO as $\Omega_{\mathrm{ind}}=2\pi L/T$ where T is the temporal period of the orbit and L is its "symbolic length" (number of returns onto the Poincaré plane). Accordingly, the value of Ω_{ind} gives the frequency per "cycle" of this UPO.

When a chaotic system is perturbed by a periodic external force, the onset of phase synchronization requires that each UPO is phase-locked with this force, and the locking ratio is the same for all of them [4]. If the individual frequencies of all UPOs in the unperturbed attractor concentrate near a certain mean value (as is the case of the phase-coherent Rössler attractor), a moderate perturbation with the close frequency is able to enforce lockings in the ratio 1:1 and, thereby, invoke phase synchronization. If, in contrast, the distribution of Ω_{ind} is sufficiently broad, the state of phase synchronization may turn unreachable. UPOs with different locking ratios coexist within the perturbed attractor, and passage of a chaotic trajectory near such UPOs results in inevitable phase jumps. The periodically forced Lorenz equations belong to the latter class; here the alternation of locking ratios brings about a so-called "imperfect phase synchronization" [5,6].

When two chaotic systems are weakly coupled, interactions between the respective UPOs create in the common phase space the countable set of unstable 2-tori (direct product of each UPO from the first system with each UPO from the second one). Transition to phase synchronization is related to onset of frequency lockings on these tori [7]. Obviously, the narrow distribution of frequencies facilitates the locking process whereas the broad distribution hampers it and makes it hardly reachable.

A convenient way to influence the temporal coherency of the flow without disturbing the geometry of the phase space is to introduce the coordinate-dependent modulation of the velocity with which the system moves along the orbit through the phase space.

Take two autonomous dynamical systems: a flow

$$\dot{\boldsymbol{x}} = \boldsymbol{F}(\boldsymbol{x}), \quad \boldsymbol{x} = (x_1, x_2, \ldots, x_N)$$

with a vector function $\boldsymbol{F}(\boldsymbol{x})$, and a flow

$$\dot{\boldsymbol{y}} = \boldsymbol{F}(\boldsymbol{y})\tau(\boldsymbol{y}), \quad \boldsymbol{y} = (y_1, y_2, \ldots, y_N)$$

where a scalar function $\tau(\boldsymbol{y})$ is positively defined (or, at least, is positive in the physically relevant part of the phase space).

Since each solution curve of the first flow is simultaneously the solution curve of the second flow and vice versa, two dynamical systems share, of course, the complete structure of the phase space. Their dynamics in time can be viewed as parametric representations of solution curves; since parameterizations are different, the same segments of solution curves are traversed by two flows with different "speed." Qualitatively, the location of all invariant objects (closed orbits, stable and unstable manifolds) is independent of the way the time is measured. The same refers to geometric quantitative characteristics of the set: Floquet eigenvalues of periodic orbits, box-counting fractal dimension of attractors, etc. [15].

Multiplication of the right-hand side by $\tau(\boldsymbol{y})$ should be understood as the coordinate-dependent reparameterization of time units. By varying the functional dependence in τ, we are able to manipulate the local speed: accelerate the passage through certain regions of the phase space and slow down the motion through other regions. This, in turn, can influence the temporal coherency. The utmost gain in the coherency would be produced by a transformation which makes the returns onto a Poincaré plane equidistant and turns the hitherto nonisochronous flow into a suspension over the Poincaré mapping. For a generic flow, such $\tau(\boldsymbol{y})$ probably does not exist. Nevertheless, it is possible to find a broad class of reparameterizations which ensure rather narrow distributions of characteristic time scales. An appropriate reparameterization can also work in the opposite direction: a function $\tau(\boldsymbol{y})$ which is close to zero on a certain small region of the attractor and relatively large elsewhere, would disrupt the temporal coherency.

In the following sections we exemplify both effects: turn the strongly nonisochronous Lorenz attractor into the temporally coherent one, and destroy the high temporal coherency of the Rössler attractor. Once the temporal characteristics of individual chaotic oscillators are changed, their ability or inability to synchronize under coupling their phases is also strongly affected.

III. HOW TO PHASE-SYNCHRONIZE TWO LORENZ ATTRACTORS

We start our demonstration with the situation where phase synchronization is allegedly impossible: the case of coupled Lorenz attractors. The well-known set of equations, derived initially in the context of atmospheric convection [8], reads as

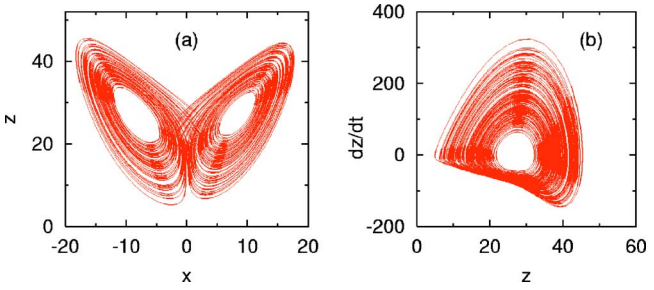

FIG. 1. (Color online) Attracting set of the Lorenz equations. (a) Double scroll in the (x,z) projection and (b) single scroll in the $(z,\dot{z})$ projection. Here and below coordinates and time units are dimensionless.

$$\dot{x} = \sigma(y - x),$$

$$\dot{y} = rx - y - xz,$$

$$\dot{z} = xy - bz, \tag{1}$$

where the parameter values $\sigma=10$, $r=28$, and $b=8/3$ from the original paper [8] (employed also for the study of synchronizability in [3]) ensure the chaotic character of dynamics. For this set of parameters the equations (1) possess the attracting set which is mirror-symmetric with respect to the transformation $(x,y)\leftrightarrow(-x,-y)$. Of three equilibrium points only the trivial state $x=y=z=0$ belongs to the attractor; two saddle-foci with coordinates $x_s^2=y_s^2=b(r-1)$, $z_s=r-1$ lie outside the attractor.

A familiar projection of the Lorenz attractor in Fig. 1(a) presents two lobes ("scrolls" in the terminology of [3]). A chaotic orbit consists of alternating segments of spiraling motions (respectively, clockwise or counterclockwise) along those scrolls. The segments are separated by passages through the "switching region" during which the sign of x changes. For an observer who follows the time evolution of the variable z, the convenient coordinates for the phase portrait are z and $\dot{z}$. In these coordinates the projection of the attractor acquires the shape of the single (deformed) scroll with the hole in the middle [Fig. 1(b)]. The orbit rotates counterclockwise along the scroll, there are no switchings, and the definition of phase as a polar angle is straightforward. However, this does not help much with respect to phase synchronization: as correctly stated in [3], the phases of two coupled systems (1) remain unlocked irrespective of the amplitude of the coupling term. This holds not only for the case of the parameter mismatch between the systems, but also for coupled identical Lorenz oscillators: their phases "drift away" from each other.

Let us perform in Eqs. (1) the coordinate-dependent rescaling of the time variable. On introducing the new "time unit" $\tau(x,y,z)$ the equations turn into

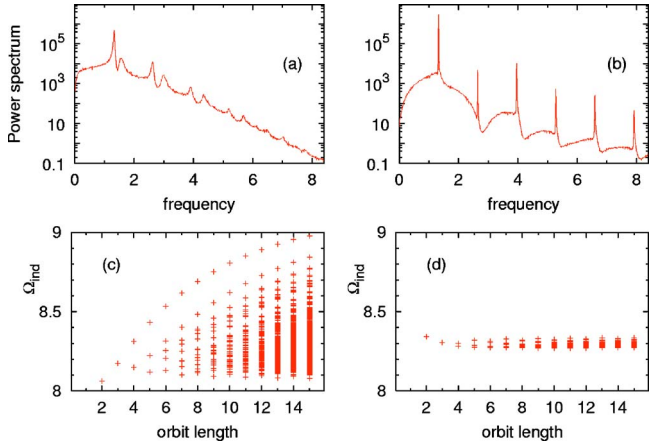

FIG. 2. (Color online) Comparison of temporal characteristics for the conventional Lorenz equations (left column) and equations with reparameterized time (right column). (a) and (b) Power spectra of the variable z for a chaotic orbit (arbitrary units). (c) and (d) Distribution of individual frequencies for UPOs embedded in the attractor.

$$\dot{x} = \sigma(y - x)\tau(x,y,z),$$

$$\dot{y} = (rx - y - xz)\tau(x,y,z),$$

$$\dot{z} = (xy - bz)\tau(x,y,z). \tag{2}$$

Our particular choice for $\tau(x,y,z)$ is the continuous nonnegative function

$$\tau(x,y,z) = 8.5\sqrt{\frac{x^2+y^2+x_s^2+y_s^2+(z-z_s)^2-2x_s|x+y|}{\sigma^2(y-x)^2+[x(r-z)-y]^2+(xy-bz)^2}}. \tag{3}$$

The denominator of $\tau(x,y,z)$ is the absolute value of the velocity vector in the phase space of Eq. (1). A division of the right-hand side of Eq. (1) by this value normalizes the velocity and turns it everywhere into the unit vector. The numerator under the square root is merely the distance from the point (x,y,z) to the nearest saddle-focus. A multiplication with this distance regularizes rotations along the scrolls, bringing them somewhat closer to isochronous "solid body rotations." Finally, the purpose of the dynamically irrelevant constant factor 8.5 (found by numerical trial) is to equalize the mean rotation rates: within a sufficiently long time interval the orbits of Eqs. (1) and (2) perform in the phase space approximately the same number of turns.

Dynamical systems defined by Eqs. (1) and (2) possess the very same attracting set: the familiar Lorenz attractor [8]. This is ensured by the fact that the direction of time is nowhere reversed: on the attractor, the function $\tau(x,y,z)$ is positive, it vanishes only in the saddle-foci points which stay outside. Furthermore, since each trajectory of Eq. (1) is a trajectory of Eq. (2) and vice versa, the Poincaré mapping induced by the flow on an appropriate secant plane also stays intact. Therefore, all accurate conclusions on the chaotic properties of trajectories drawn from the rigorous analysis of this mapping (see, e.g., [9–11]) remain valid.

However, the dynamics governed by Eq. (2) is much more temporally coherent than on the classical Lorenz attractor. This is demonstrated in Figs. 2(a) and 2(b) which show the power spectra of the variable z taken from a chaotic orbit. For the case of nonparameterized time, the main peak in the power spectrum is moderate. For Eq. (2) this peak is much sharper: it is higher than the background by four orders of magnitude.

Characterization of dynamics in terms of individual frequencies of unstable periodic orbits embedded in the attractor also indicates the high degree of temporal coherency for dynamics with the time reparameterized. The lower panel of Fig. 2 presents the distributions of individual frequencies for all 4665 UPOs with symbolic length (number of turns in the phase space) $\leqslant 15$ embedded in the Lorenz attractor. For the conventional Lorenz equations (1) the distribution is quite broad [Fig. 2(c)]; its width exceeds 10% of the mean frequency of the chaotic motion 8.365…. In contrast, the equations with reparameterized time yield for the individual frequencies the narrow distribution shown in Fig. 2(d); its width is less than 1% of the mean frequency.

Having turned the dynamics into the temporally coherent one, we can proceed to coupling two such sets of equations. Both the structure of the coupling term and its place in the set are of certain relevance. The term proportional to the difference between x_1 and x_2, as employed in [3], is not very helpful: for the variant of "in-phase" state in which the subsystems are located on the opposite scrolls, such coupling plays the desynchronizing role. Instead, one might utilize the mirror symmetry of the system by using the squared values of x or y, e.g., $dx_1^2/dt = \cdots + \varepsilon(x_2^2 - x_1^2)$. The latter, however, cannot be viewed as a uniformly weak coupling: it adds to the equation for dx_1/dt the term $\sim x_2^2/x_1$ which diverges during the switch from one scroll to another. The proper way appears to be the introduction of the coupling term in the equations for the variable z:

$$\begin{aligned}
\dot{x}_1 &= \sigma_1(y_1 - x_1)\tau(x_1, y_1, z_1), \\
\dot{y}_1 &= (rx_1 - y_1 - x_1 z_1)\tau(x_1, y_1, z_1), \\
\dot{z}_1 &= (x_1 y_1 - b z_1)\tau(x_1, y_1, z_1) + \varepsilon(z_2 - z_1), \\
\dot{x}_2 &= \sigma_2(y_2 - x_2)\tau(x_2, y_2, z_2), \\
\dot{y}_2 &= (rx_2 - y_2 - x_2 z_2)\tau(x_2, y_2, z_2), \\
\dot{z}_2 &= (x_2 y_2 - b z_2)\tau(x_2, y_2, z_2) + \varepsilon(z_1 - z_2). \qquad (4)
\end{aligned}$$

We employ the same parameter values $r=28$ and $b=8/3$ as above. To introduce the parameter mismatch between the systems, we take different values of the parameter σ: $\sigma_1 = 10$ and $\sigma_2 = 11$ (the same values were used by the authors of [3]). Numerical simulation of Eq. (4) has shown that the state of phase synchronization can be reached at quite modest values of the coupling strength ε: for $\varepsilon \geqslant 0.11$ we did not observe jumps in the phase difference. This holds for all three basic algorithms of computing the phase [1]: the polar angle on the coordinate plane spanned by $z - z_s$ and $\dot{z}$, the linear interpolation between the moments of intersection of the Poincaré surface (the standard choice: plane $z = r - 1$) and the phase of the analytic signal recovered with the help of the Hilbert transform.

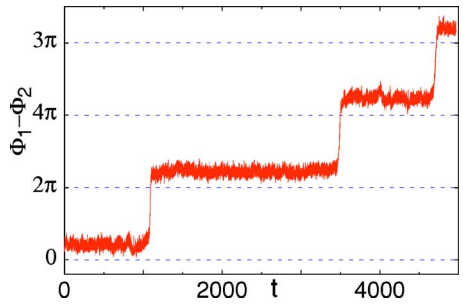

FIG. 3. (Color online) Growth of phase difference between the subsystems of Eq. (4) at $\varepsilon = 0.1072$. Phases Φ_1 and Φ_2 are reconstructed by means of the Hilbert transform.

Evolution of phase difference just below the onset of phase synchronization is presented in Fig. 3: the long epochs of phase-synchronized motion, which spread over thousands of turns in the phase space, are separated by relatively short intervals during which the phase difference increases by 2π.

Visual inspection of phase portraits in Figs. 4(a) and 1(a) discloses no noticeable differences. This allows us to view the coupling, required for the onset of phase synchronization, as weak: it does not introduce substantial changes into the structure of the attractor. The amplitudes remain largely decoupled; this can be seen in Fig. 4(b) which shows chaotic evolution of the difference $x_1 - x_2$. We see that epochs when both trajectories rotate in half-spaces with the same sign of x alternate with segments when the sign of x in two subsystems is different.

The outcome of this numerical experiment tells us unambiguously: phase synchronization between coupled geometric attractors with several scrolls is possible.

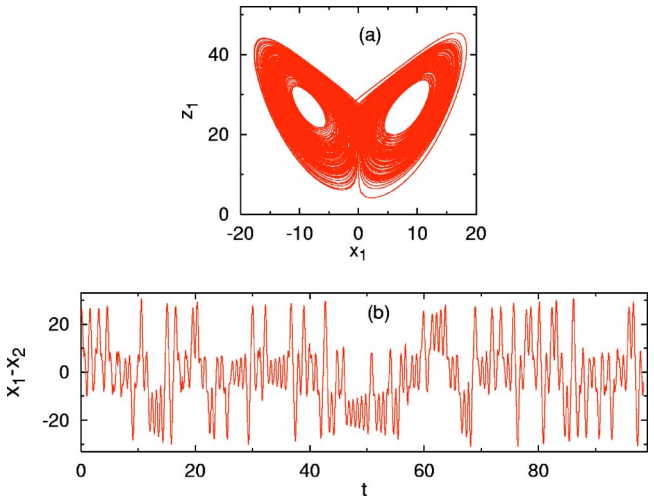

FIG. 4. (Color online) Dynamics of Eq. (4) in the state of phase synchronization at $\varepsilon = 0.11$. (a) Projection of the attractor on the plane (x_1, z_1) and (b) temporal evolution of $x_1 - x_2$.

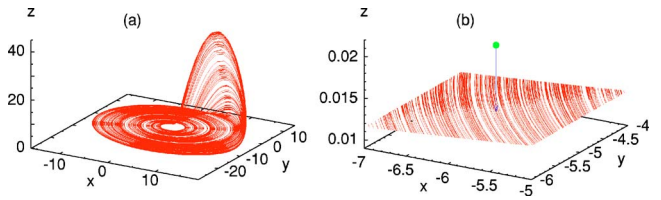

FIG. 5. (Color online) (a) Rössler attractor in the phase space: $a=0.165$, $b=0.2$, $c=10$, and $\omega=0.99$. (b) Position of the added "slow" point with respect to the attractor of the Rössler equations.

IV. HOW TO DESYNCHRONIZE TWO RÖSSLER ATTRACTORS

In this section the coordinate-dependent reparameterization of time brings about the opposite effect: it destroys temporal coherency and disables phase synchronization. For this purpose we take the system of two coupled chaotic Rössler oscillators [12]

$$\begin{aligned}
\dot{x}_1 &= (-\omega_1 y_1 - z_1)\tau(x_1,y_1,z_1) + \varepsilon(x_2 - x_1),\\
\dot{y}_1 &= (\omega_1 x_1 - a y_1)\tau(x_1,y_1,z_1),\\
\dot{z}_1 &= [b + z_1(x_1 - c)]\tau(x_1,y_1,z_1),\\
\dot{x}_2 &= (-\omega_2 y_2 - z_2)\tau(x_2,y_2,z_2) + \varepsilon(x_1 - x_2),\\
\dot{y}_2 &= (\omega_2 x_2 - a y_2)\tau(x_2,y_2,z_2),\\
\dot{z}_2 &= [b + z_2(x_2 - c)]\tau(x_2,y_2,z_2),
\end{aligned} \tag{5}$$

with parameter values $a=0.165$, $b=0.2$, $c=10$, $\omega_1=0.95$, and $\omega_2=0.99$. Without coupling ($\varepsilon=0$) both individual subunits exhibit chaotic oscillations.

For the conventional choice of time scale $\tau(x,y,z)\equiv 1$, those chaotic oscillations are nearly isochronous. The mean frequencies of two attractors are slightly different, due to the difference between the values of $\omega_{1,2}$. Equations (5) with this set of parameter values and $\tau=1$ were used for the first description of chaotic phase synchronization in [2]. A rather weak coupling suffices for bringing the phases of two systems together: for $\varepsilon > 0.0417$ no phase jumps were observed [7].

The high degree of temporal coherency in the Rössler attractor makes it difficult to resolve the fine details of transition to phase synchronization, therefore the authors of [13] had to reduce it with the help of the mildly varying τ. We introduce a stronger disturbance which aims at destruction of the phase synchronization.

The Rössler attractor, in its large parts, has a shape of a thin disk which is nearly parallel to the x,y plane [Fig. 5(a)]. For reparameterization of time, we choose the function

$$\tau(x,y,z) = C[(x-x_0)^2 + (y-y_0)^2 + (z-z_0)^2 + d_0], \tag{6}$$

where C and d_0 are non-negative constants and (x_0,y_0,z_0) are the coordinates of the point which lies slightly *outside* the attractor. We take the values $x_0=-6$, $y_0=-5$, and $z_0=0.02$, i.e., slightly beyond the disk. Location of this point with respect to the attractor is shown in Fig. 5(b); its distance from the nearest place on the attractor is of the order 0.01. During the passages close to this point, the system slows down and hovers for the long time in its vicinity; in the distant parts of the attractor, on the opposite, the factor $\tau(x,y,z)$ serves for the strong increase of the local velocity along the trajectory. Further, we fix the value $d_0=0.01$ so that the function $\tau(x,y,z)$ nowhere vanishes. Finally, to make the mean frequency of chaotic oscillations in the reparameterized system approximately equal with that of the conventional Rössler attractor, we set $C=0.035$.

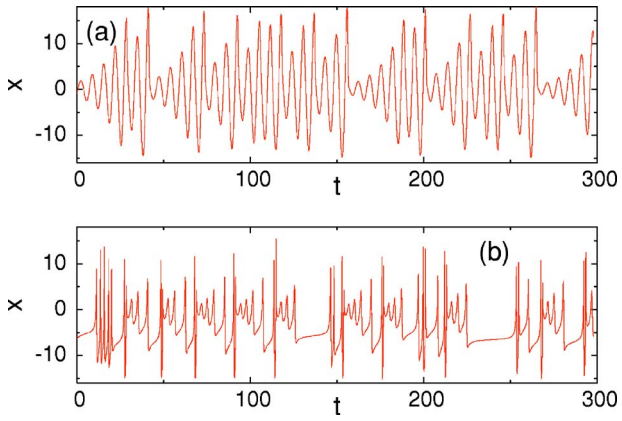

FIG. 6. (Color online) Time series of the variable x on the Rössler attractor. (a) conventional time and (b) time reparameterized according to Eq. (6). Coordinates and time units are dimensionless.

Figure 6 shows the effect of time reparameterization on the temporal dynamics. In the upper panel which presents the evolution of the variable x for conventional time ($\tau=1$), the oscillations have approximately constant period and modulated amplitude. The lower panel shows the segment of the very same chaotic orbit which is traversed in the reparameterized time. Very fast oscillations alternate here with relatively long epochs of hovering during the passages close to the "slow" point. Of course, evolution of the phase is here very inhomogeneous: during the hovering intervals the phase remains nearly constant, whereas the rate of its growth in the distant parts of the attractor is rather high.

The difference between the characteristics of coherency on the Rössler attractor for two different functions τ is summarized in Fig. 7. The left column corresponds to $\tau=1$ (no reparameterization). This is definitely a case of high temporal coherency: in the power spectrum the main sharp peak exceeds the background by three orders of magnitude, and the distribution of individual frequencies of unstable periodic orbits is very narrow: all values lie in the small interval between 0.960 and 0.993.

The right column shows the same characteristics after the reparameterization of time. The power spectrum lacks outstanding peaks, and the distribution of individual frequencies for UPOs is rather broad, ranging from 0.57 to 2.76.

Since temporal coherency is apparently destroyed by the reparameterization (6), we were unable to observe the state of phase synchronization in Eq. (5) at small or moderate values of the coupling strength ε. This failure does not de-

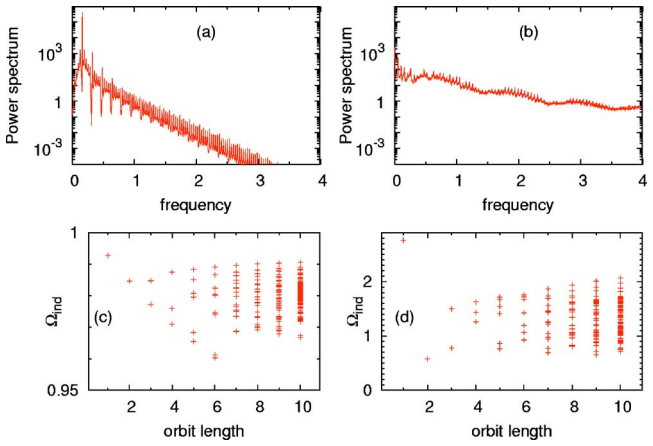

FIG. 7. (Color online) Comparison of temporal characteristics for the conventional Rössler equations (left column) and the same equations with time reparameterized according to Eq. (6) (right column). (a) and (b) Power spectra of the variable x for a chaotic orbit (arbitrary units). (c) and (d) Distribution of individual frequencies for UPOs embedded in the attractor.

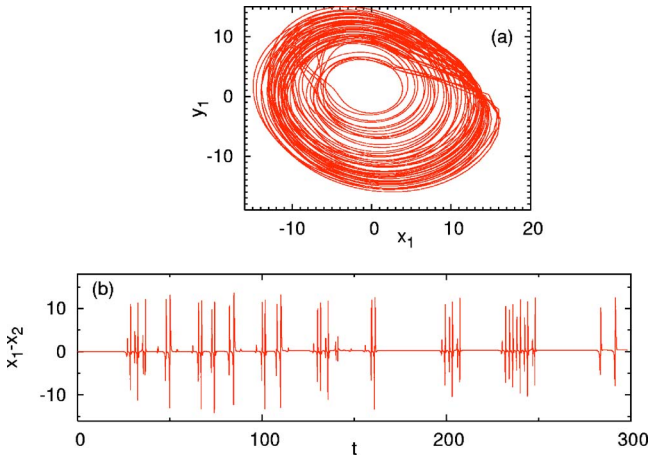

FIG. 8. (Color online) Synchronized state at $\varepsilon=2.58$: (a) Projection of the phase portrait for one of the oscillators and (b) on-off intermittency in the evolution of x_1-x_2. Coordinates and time units are dimensionless.

pend on the method by which the phase was evaluated: neither the phases computed through the Hilbert transform nor the phases as polar angles on the planes x_1,y_1 and x_2,y_2 nor the phases obtained by interpolation between the returns onto the Poincaré planes $y_{1,2}=0$ exhibit the visible tendency to entrainment.

The difference between the phases remains unbounded for $\varepsilon<\varepsilon_c=2.58$. Beyond ε_c the phases are entrained. This is, however, already a very strong coupling which noticeably distorts the attractors [cf. the "flight" segments in the left part of Fig. 8(a) where one of the oscillators virtually drags the other one away from the region of the slow point].

The state which is reached at high values of ε cannot be properly classified as phase-synchronized, since the amplitudes are not uncorrelated anymore. We draw this conclusion from the temporal evolution of x_1-x_2 in Fig. 8(b). The apparent regime of on-off intermittency implies that the oscillators are not very far from being completely synchronized.

If, instead of $d_0=0.01$, we set the minimal value of $\tau(x,y,z)$ in Eq. (6) at $d_0=0$, enhancing thereby the slowdown effect, the state of chaotic synchronization becomes practically unreachable: two attractors synchronize only at still higher values of ε when the shape of the attractor becomes very strongly deformed, and the further minor increase of ε replaces chaos by periodic oscillations.

The result of this experiment shows that the appropriate coordinate-dependent reparameterization of time can disrupt phase synchronization between two similar chaotic oscillators in spite of the very "convenient" geometry of their attractors.

V. DISCUSSION

Our examples demonstrate that given only the shape of the attractor, we cannot decide whether a corresponding chaotic oscillator, when coupled to other similar objects, can easily synchronize its pace with their rhythms. Much more important in this respect is the presence or absence of a characteristic time scale, the circumstance determined not so much by the shape of the attractor as by the peculiarities of the motion along it. By accelerating or decelerating this motion in proper regions of the attractor, it is possible to alter substantially the characteristics of temporal coherency, and thereby to influence the very possibility of the transition to phase synchronization. Reparameterizing functions τ can be taken from the broad classes of functions; the above examples of τ are, of course, neither exceptional nor optimal (in the sense, say, of enabling chaotic phase synchronization at the lowest value of the coupling strength).

We should not, however, overestimate the significance of these formal examples. Of course, it would be very attractive to use coordinate-dependent reparameterization of time as a tool which facilitates the onset of desirable phase synchronization (e.g., for increasing the output of a network) or suppresses the harmful synchrony (e.g., in neurons of Parkinsonic patients). Given the explicit dynamical equations, the choice of the appropriate time reparameterization is not a very difficult task. However, one should be aware that all accelerations and/or hoverings take place in the abstract phase space, whereas the experimentally available possibilities to influence a physical (biological, etc.) system are restricted to the real world. Modifying a given physical object in such a way that in its mathematical model all phase trajectories remain intact but the speed along them changes, may prove to be a problem without a feasible solution.

ACKNOWLEDGMENTS

M.Z. acknowledges the support of Sonderforschungsbereich 555. E.-H.P. thanks the financial support provided by NIH Grant No. NS40785-03.

[1] A. Pikovsky, M. Rosenblum, and J. Kurths, *Synchronization: A Universal Concept in Nonlinear Sciences* (Cambridge University Press, Cambridge, 2001).
[2] M. G. Rosenblum, A. S. Pikovsky, and J. Kurths, Phys. Rev. Lett. **76**, 1804 (1996).
[3] L. Zhao, Y. C. Lai, R. Wang, and J. Y. Gao, Europhys. Lett. **66**, 324 (2004).
[4] A. Pikovsky, G. Osipov, M. Rosenblum, M. Zaks, and J. Kurths, Phys. Rev. Lett. **79**, 47 (1997).
[5] M. A. Zaks, E.-H. Park, M. G. Rosenblum, and J. Kurths, Phys. Rev. Lett. **82**, 4228 (1999).
[6] E.-H. Park, M. A. Zaks, and J. Kurths, Phys. Rev. E **60**, 6627 (1999).
[7] D. Pazó, M. A. Zaks, and J. Kurths, Chaos **13**, 309 (2003).
[8] E. N. Lorenz, J. Atmos. Sci. **20**, 130 (1963).
[9] V. S. Afraimovich, V. V. Bykov, and L. P. Shilnikov, Sov. Phys. Dokl. **22**, 253 (1977).
[10] J. Guckenheimer and R. F. Williams, Publ. Math., Inst. Hautes Études Sci. **50**, 59 (1979).
[11] J. A. Yorke and E. D. Yorke, J. Stat. Phys. **21**, 263 (1979).
[12] O. E. Rössler, Phys. Lett. **57A**, 397 (1976).
[13] E. Rosa, E. Ott, and M. H. Hess, Phys. Rev. Lett. **80**, 1642 (1998).
[14] Of course, the distribution of characteristic times on the attracting set is not completely independent from its geometry: thus passages near saddle-points or saddle-foci in the attractor of the smooth flow are rather (logarithmically) long.
[15] On the contrary, Floquet exponents, Lyapunov exponents, and similar characteristics measured in terms of direct or inverse time units, depend, of course, on the choice of the time scale.